C.P. No. 492
(20,361)
A.R.C. Technical Report

C.P. No. 492
(20,361)
A.R.C. Technical Report

MINISTRY OF AVIATION

AERONAUTICAL RESEARCH COUNCIL

CURRENT PAPERS

A Turbine Nozzle Cascade for cooling Studies. Part 1. The Measurement of Mean Nusselt Numbers at the Blade Surface.

By

R. I. Hodge

LONDON: HER MAJESTY'S STATIONERY OFFICE

1960

FOUR SHILLINGS NET

U.D.C. No.621.438-71:536.244 C.P. No. 492

Memorandum No. M.308

NATIONAL GAS TURBINE ESTABLISHMENT

A turbine nozzle cascade for cooling studies Part I: The measurement of mean Nusselt numbers at the blade surface

- by -

R. I. Hodge

May, 1958

SUMMARY

A description is given of a cascade tunnel designed and built to evaluate various cooling systems for turbine blading. Details of the tunnel instrumentation and operating conditions are included.

Gas to blade surface mean heat transfer coefficients have been determined in tests using a special blade. These experimental coefficients are related to blade Reynolds number and to the temperature ratio between gas and blade surface.

The second part to the present pair of Memoranda compares these experimental results with predicted values.

CONTENTS

TABLE

ILLUSTRATIONS

1.0 Introduction

The development of gas turbine engines for aircraft propulsion has led to the use of gas temperatures which necessitate cooling of the turbine components in particular the blading. Thus in the design stage of a projected engine, blade temperatures and coolant requirements have to be estimated at varying operating conditions. To test the utility of estimating procedures, they may be used and compared with performance results from rig investigations using adequately instrumented test blades. These investigations are much simplified when the effects of rotation are not included and the blades are mounted in static cascades.

In one of the cascade tunnels installed at this Establishment for such use, the blade profiles were typical of cooled nozzle guide vanes. The present series of Memoranda (in two parts) describe this rig (the No. 4 High Temperature Tunnel), and give details both of its equipment and its performance.

A specific aspect of performance which is of particular interest in a cascade designed for blade cooling studies is the gas to blade convective heat transfer. The estimation of cooled blade material temperatures, coolant distribution and temperature rise when the surface pattern of gas to blade heat transfer rates is known, is a laborious computational process. The calculation is much simplified when chordwise perimeter averages are assumed to be effective in the basic equations[1,2]. The main burden of this pair of Memoranda is therefore the surface mean heat transfer coefficients obtaining at various gas flow conditions: Part I deals with the measured values, and Part II gives a comparison with predicted rates.

2.0 Apparatus and method

An external view of the No. 4 High Temperature Tunnel installation, with the rig partially dismantled, is given in Figure 1. The gas flow was directly heated, when required, by using one or both of the parallel combustion chambers. These chambers have outlet scoops, projecting into the refractory lined mixing box, which served to deflect the two streams towards each other. The mixed flow entered the cascade through a pair of gauzes followed by a parallel section some six chords long. The installation was designed to deliver gas flows to the cascade sufficient to cover the range[3]:-

Gas total temperature - 20 → 1000°C

Mach number at blade exit - up to 1

Blade exit static pressure - approximately atmospheric

2.1 The cascade tunnel

The tunnel was equipped with blades to the profile shown in Figure 2, set at zero inlet angle: the measurements were restricted to this profile at zero incidence. The cascade geometry was as follows:-

chord, c	2.23 in.
pitch, s	1.46 in. ; s/c = 0.65
span, ℓ	4.5 in. ; ℓ/c = 2.02
design gas outlet angle, $\bar{\alpha}_2$	62°

The blades were all carried in cantilever fashion, there being a clearance between their tips and the adjacent wall: this measured 0.1 in. at the test blade position and 0.05 in. in the case of the permanent blades. The test blade was carried in the wall seen in Figure 3, the others being fixed in the opposite wall.

The side walls and fixed blades had internal passages coupled into two circuits, through which cooling air or water could be circulated. In these tests both circuits were fed from the water main. The four dummy blades adjacent to the test position were provided with thermocouples on the surfaces facing the test blade. In this way radiation losses could be assessed. The test blade root was insulated from the cooled wall in which it was accommodated by an insulating liner $\frac{1}{4}$ in. thick, to reduce conduction losses.

The tunnel carried a variety of instruments on its entry and exit components: these are indicated in Figure 3. Around the wall of the entry section eleven static points were manifolded together. Stagnation thermocouples and pitot tubes which protruded to the quarter span depth were carried on the entry side walls. Another stagnation thermocouple which could be traversed the depth of the tunnel gave the mid-span temperature distribution. Three pairs of opposite static holes were drilled in the exit side walls. A pitot yawmeter could be rotated and traversed vertically at various span depths close to the blade outlets. On the roof of the exit section a probe holder at mid-span had freedom of movement in the two ways to allow a pitot tube to be fed over the surfaces of the test blade.

For the preliminary inlet velocity and temperature traverses reported in a later section, additional instruments spanning the tunnel were fitted in place of the pair of entry pitot tubes. These manually-traversable instruments had extended ends so that the blockage introduced was constant during the traverse.

2.2 The test blade

The gas to blade heat flow was measured on the test blade shown in Figure 4. A separate flow of coolant was passed through the profile, and from recorded flow rates, temperature rise, mean profile temperature, gas temperature and a knowledge of the specific heat of the coolant and the measured surface area, the profile surface mean heat transfer coefficient was deduced.

The profile was made of copper to reduce surface temperature variation to a minimum. Point measurements of this temperature were made at four positions at mid-span and it was assumed that the perimeter mean of these readings was the effective average for the entire surface. The surface thermocouples consisted of constantan wires carried inside copper tubes 0.059 in. o.d., 0.031 in. i.d. These tubes were brazed into grooves

in the blade from mid-span to root, thus avoiding the local cooling about the measuring point which would have resulted had the leads been brought out directly into the coolant passages.

Mains water was used as a coolant, having a temperature at entry to the blade of about 20°C. It was passed into and out of the blade through measuring stations which were reverse flow jacketed to give a well mixed flow over the thermometer. The external assembly was lagged and jacketed to prevent heat losses. A reverse flow system about the thermometer at the outlet station was a further safeguard. The mercury-in-glass 0 to 50°C thermometers were graduated in tenths of a degree, and with flow rates adjusted to give temperature rises of about 10°C it was expected that an accuracy of not worse than ±2 per cent could be achieved. If local boiling were to occur within the profile the possibility of unaccounted heat flow arises, due to the escape of steam through the outlet station. To prevent this possibility it was stipulated that the measured profile surface temperatures should all be at least 10°C below the boiling point of the coolant. As a result of these limitations and of the relatively high water inlet temperature, the range of the tests was restricted to a temperature ratio, gas to mean blade surface, from about 1.2 to 1.9.

The weight rate of flow of the coolant was determined by intermittently timing the passage of a certain quantity. The time interval was never less than one minute so that an accuracy of better than 1 per cent could be easily obtained.

Losses from the heated profile by way of the exposed root fitments were obviated by having a second water circuit in the root block. This was fed with the warm water leaving the profile circuit, after passing through the outlet temperature measuring station.

Those surfaces which were exposed to the gas flow and whose background was in contact with the profile circuit coolant were measured and used to determine the heat transfer coefficient. The profile area, tip area and a proportion of the root platform surface were summed to give the 0.162 ft^2 used in the calculation.

3.0 Test results

3.1 Tunnel entry gas flow conditions

The cascade may be supplied in one of four different ways; for low temperatures the uncooled facility compressor outlet temperature may be adequate; for intermediate temperature one of the two combustion chambers may be used; for temperatures exceeding about 500°C, both chambers must be used, although their combined use may be extended down to about 350°C.

The cascade entry was fitted with a pair of gauzes providing a 45 per cent and 40 per cent blockage in close series with a combined projected blockage ratio of more than 90 per cent, but nevertheless distinctive total pressure, incidence and temperature distributions varying with the use of the optional gas supplies were apparent.

3.1.1 Incidence

Incidence variations were examined at one overall condition, i.e. a flow to give a mean blade outlet Mach number $M_2 = 0.77$ and a gas total temperature of 350°C. These distributions are plotted in Figure 5.

Since No. 1 combustion chamber was on the test blade tip side of the mixing box it is obvious that the preferential circulation in the mixing box was of the direction which would result from flow through this combustion chamber alone. When No. 2 chamber was used the heat addition caused a reversal of this circulation. The incidence pattern with both chambers in operation indicated a very weak resultant circulation in the preferential direction.

Incidence changes within the range detected are not likely to affect the blade performance materially, except perhaps near the tip with No. 2 combustion chamber alight. Incidences greater than $+10^{\circ}$ may modify the pressure distribution around the convex surface to an extent sufficient to move the point of separation or transition a small distance. This possibility is taken up in Part II of the present series.

3.1.2 Temperature

Temperature patterns were obtained at a combustion temperature rise of about $330^{\circ}C$ for the three modes of hot operation over a wide range of flows. The plots are given in Figure 6. It appears that flow rate did not affect the distribution. Rather surprisingly the peak temperatures were observed inboard of mid-span at all modes of operation.

The scale of variation from centre line temperature expressed as a proportion of combustion temperature rise is superimposed on the plot. Although no experimental verification was obtained it is expected that this is likely to be the significant parameter.

In cooled blade studies it is convenient to express temperatures relative to the interval between gas effective temperature T_g, and coolant entry temperature, T_c: for example a blade surface temperature T_b would become $\frac{T_b - T_c}{T_g - T_c}$. The difference $T_g - T_c$ is in fact combustion temperature rise. Thus the proportional variation in temperature shown in Figure 6 would show up as a reciprocal effect on a particular temperature expressed relatively. Since there are reasons for desiring cooling studies to be accurate to within ± 0.01 on the relative temperature scale, the observed temperature variation may be significant.

3.1.3 Total pressure

It was assumed that the static pressure remained sensibly constant across the test blade span, in the cascade entry. The results of total pressure traverses, presented as point velocity heads compared with entry mean velocity head calculated on this supposition, are given in Figure 7. In the lower graph, traverses at flows giving blade outlet Mach numbers about 0.77 are compared for the three modes of hot operation: in each case the temperature was maintained at about $350^{\circ}C$. In the upper graph the effects of flow rate are compared for the cold mode of operation, at a gas temperature of approximately $120^{\circ}C$.

It will be observed that the rotating flow produced velocity peaks within the inner and outer quarters of the blade span: heat addition in No. 2 combustion chamber displaced the pattern of relative peaks apparent in the other modes. Increasing flow caused small increases in the peak values.

The velocity head variation will not alter gas to blade heat transfer coefficients very much. Assuming for example that the relevant Nusselt number is proportional to Reynolds number raised to the 0.6 power, then a 20 per cent increase in velocity head produces less than 6 per cent increase in heat transfer coefficient.

3.2 Heat transfer measurements

In the measurement of mean surface heat transfer coefficient the effect of variations in gas distribution at entry to the test blade must be considered. The low temperature results were obtained in tests without combustion, where the temperature must have been nearly uniform and the mid-span velocity was practically equal to the average across the test blade span. For the remainder of the tests No. 2 combustion chamber was used: this gave a centre line temperature fairly near the bulk mean, but at mid-span a trough in the velocity head profile was apparent, corresponding to about 6 per cent reduction in heat transfer coefficient. The conductivity of the copper blade was relied upon to smooth out this irregularity of coefficient distribution and, judging by the way blade temperatures are shown in Table I to be relatively unaffected by major changes in gas temperature, this supposition seems tenable.

The results are expressed non-dimensionally as Nusselt number, Reynolds number and gas to blade temperature ratio. The heat transfer coefficient, $\bar{h}$, was deduced from Q, the heat flow rate, the effective area, A, and the temperature difference, (gas effective - blade surface mean). Thus:-

$$\bar{h} = \frac{Q}{A(T_g - \bar{T}_b)} \qquad \ldots \quad \ldots \quad (1)$$

It is expressed as a Nusselt number:-

$$\bar{N}u = \frac{\bar{h}\, c}{\lambda} \qquad \ldots \quad \ldots \quad (2)$$

where c is the chord of the blade and λ the conductivity of the gas measured at the gas effective temperature. It was assumed that the gas flow conditions were controlled by the Reynolds number, and that effects due to compressibility were negligible. Reynolds number is expressed as:-

$$R_2 = \frac{W_g c}{A_t \mu} \qquad \ldots \quad \ldots \quad (3)$$

where W_g is the gas weight flow rate, c the blade chord, A_t the throat area of the test blade passage and μ the gas viscosity measured at the gas effective temperature. The temperature ratio, gas to blade is taken as $T_g/\bar{T}_b$ where T_g is the gas effective temperature and $\bar{T}_b$ the perimeter-mean surface temperature at mid-span. The gas effective temperature used throughout is:-

$$T_g = T_1 \left(1 - \frac{0.14 \frac{\gamma - 1}{2} M_2^2}{1 + \frac{\gamma - 1}{2} M_2^2} \right) \ldots \ldots \quad (4)$$

where T_1 is the total temperature at inlet, M_2 the outlet Mach number and γ, the ratio of the specific heats. This expression is assumed to be a sufficient approximation to the surface mean stagnation temperature, (to be discussed further in Part II of the present series).

All the test results are shown in the scatter diagram, Figure 8. They were separately analysed in three categories according to the gas temperature:-

(i) less than 500°C

(ii) between 500°C and 600°C

(iii) more than 600°C.

The best lines are shown in Figure 9. The temperature ratios in each category were separately averaged and are, with their standard deviations:-

(i) 1.22 ± 0.03 (±2.5 per cent)

(ii) 1.58 ± 0.02 (±1.5 per cent)

(iii) 1.89 ± 0.02 (±1.1 per cent).

5.2.1 Temperature ratio effect

Because the physical properties of air which are relevant to the convective transfer of heat are dependent upon temperature, there is therefore an effect which can be best expressed by a power of the ratio of gas to blade temperature. The gas temperature chosen is the "effective" or the approximation to the mean stagnation temperature around the profile.

The three categories mentioned in the preceding section have been used to determine this temperature ratio effect. Any unidentified losses or heat gains would obviously have an influence on this analysis. Conduction and radiation loss out of the profile, not showing up in the heat balance, would lead to test values of Nusselt number which are lower than those obtaining. The percentage reduction in these tests would be inversely proportional to the temperature difference since the loss is likely to be nearly constant, the variation in measured blade temperature and its surrounds being negligible. Referring to Figure 9, the line for the highest temperature ratio is likely to be the most accurate and any corrections would result in an increase in Nusselt number at a given Reynolds number. A transfer of heat from the root circuit to the inlet side of the profile circuit is possible and this would require corrections in the opposite sense to that for radiation and conduction loss. Estimates show this transfer, as well as the losses, to be negligible.

The Nusselt number has been plotted against the temperature ratio for certain Reynolds numbers. The three points in each curve indicate

that, at temperature ratios near unity, Nusselt number is independent of the ratio, and at higher positive values of $T_g/\overline{T}_b$, $\frac{d\,(Nu)}{d\left(T_g/\overline{T}_b\right)} = -$ (an increasing function of $T_g/\overline{T}_b$). Plotting the values logarithmically shows a similar curve, but with the limited evidence available the logarithmic curves have been approximated in straight lines. The results are:-

$$R_2 = 2 \times 10^5 \quad , Nu \propto \left(T_g/\overline{T}_b\right)^{-0.16} \qquad \ldots \ldots \quad (5a)$$

$$3 \times 10^5 \quad , \qquad \left(T_g/\overline{T}_b\right)^{-0.14} \qquad \ldots \ldots \quad (5b)$$

$$4 \times 10^5 \quad , \qquad \left(T_g/\overline{T}_b\right)^{-0.17} \qquad \ldots \ldots \quad (5c)$$

The average value of the exponent is -0.16 and it is therefore assumed that $Nu \propto \left(T_g/\overline{T}_b\right)^{-0.16}$ over the range of the tests, $R_2 = 10^5$ to 8×10^5, $T_g/\overline{T}_b = 1$ to 2.

3.2.2 Approximations

In a design computation, it is convenient to have the expression for mean external heat transfer coefficient in a simple form[1], e.g.

$$Nu = \text{constant} \times (R_2)^x \times \left(T_g/\overline{T}_b\right)^y \qquad \ldots \ldots \quad (6)$$

The temperature ratio effect has already been deduced in the preceding section. In that analysis the approximating straight lines were extrapolated to a temperature ratio equal to unity. The Nusselt numbers at this value have been plotted in Figure 10 and a curve generally parallel to the test curves passed through them.

This curve cannot be approximated with sufficient accuracy over the test range by a single straight line. The curve displays a rapid change of slope about $R_2 = 2 \times 10^5$, therefore this has been regarded as a fixed point and two straight line approximations made from there to cover the test range. These logarithmic lines give the relationships:-

(i) for R_2 between 1.5×10^5 and 10^8

$$Nu = 322 \left(\frac{R_2}{2 \times 10^5}\right)^{0.715} \qquad \ldots \ldots \quad (7a)$$

(ii) for R_2 below 2×10^5

$$Nu = 322 \left(\frac{R_2}{2 \times 10^5}\right)^{0.463} \qquad \ldots \ldots \quad (7b)$$

The first expression approximates the curve to within +4.2 per cent between 2×10^5 and 6×10^5, being exact at those points: it is within -5 per cent at the stated limits. The second relationship is better than ±1 per cent down to $R_2 = 10^5$. It is assumed that the previously determined temperature ratio can be applied to these approximations without introducing an error greater than a further ±1 per cent.

4.0 Conclusions

In providing a wide range of gas flow rates and temperatures to the No. 4 High Temperature Tunnel, a non-uniform entry gas distribution had to be accepted. Within the test blade length between 0.1 and 0.9 span were experienced:-

(a) incidence variations of $+10^\circ$ to -8°,

(b) velocity head distribution within ±20 per cent of mean value,

(c) gas total temperature range from 1.03 to 0.97 centre line value, expressed as combustion temperature rise.

The effect of these discrepancies on gas to blade convective heat transfer is probably small: the incidence range is unlikely to alter the boundary layer development sufficiently to modify transition or separation; the velocity variation introduces at the most a ±6 per cent variation about the average in local heat transfer coefficient. The effect of the gas temperature variation is more complex: if the blade metal conductivity is high, then the mid-span value which approximates the bulk mean temperature should be chosen; for low conductivity materials, the measurement of gas temperature in line with the blade thermocouple station under consideration reduces errors to a minimum.

Mean surface heat transfer coefficients between gas and blade have been obtained in a manner which reduces the effect of gas distribution to a minimum, and they may therefore be considered representative of a uniform flow. The relevant Nusselt number-Reynolds number relation is presented in Figure 10 for a temperature ratio approaching unity: for other ratios the Nusselt number may be taken as the value at unity multiplied by $\left(T_g/T_b\right)^{-0.16}$. Within the range of the tests, Reynolds number 10^5 to 8×10^5, temperature ratio 1 to 2, Mach number 0.2 to 0.8, the accuracy of this approximation is expected to be better than ±1 per cent.

The relation may be further approximated by a simple power relationship, at $T_g/T_b \rightarrow 1$:-

(i) between Reynolds number of 1.5×10^5 and 10^6

$$Nu = 322 \left(\frac{R_2}{2 \times 10^5} \right)^{0.715} \quad \ldots \ldots \quad (7a)$$

the accuracy being within ±5 per cent,

(ii) between $R_2 = 10^5$ and 2×10^5

$$Nu = 322 \left(\frac{R_2}{2 \times 10^5} \right)^{0.463} \quad \ldots \quad \ldots \quad \ldots \quad (7b)$$

the accuracy being within ±1 per cent, and the relationship probably holding at values of R_2 below 10^5.

The temperature ratio effect of the first paragraph may also be applied to these approximations.

REFERENCES

No.	Author(s)	Title, etc.
1	D. G. Ainley	Internal air-cooling for turbine blades. A general design survey. A.R.C. R & M3013, 1957.
2	J. N. B. Livingood W. B. Brown	Analysis of spanwise temperature distribution in three types of air-cooled turbine blades. N.A.C.A. Report 994, 1950.
3	S. J. Andrews H. Ogden J. Marshall	Some experiments on an effusion cooled turbine nozzle blade. A.R.C. Current Paper 17,890, May 1954.

TABLE I

Heat transfer test results

Test No.	Reynolds number R_{e_2} based on mass flow, blade dimensions, effective gas temperature	Effective gas temp. T_g °K	Outlet Mach number M_2	Mean blade temperature T_b °K	Nusselt number Nu based on profile + tip + ½ root platform area, blade chord, effective gas temperature
3	7.847 × 10^5	392	0.815	327	890
	3.536 "	387	0.391	318	472
	1.885 "	350	0.186	312	303
4	4.625 "	386	0.527	322	583
	6.318 "	399	0.709	321	704
	1.263 "	509	0.198	322	247
5	1.254 "	509	0.196	319	244
	1.255 "	507	0.197	320	254
	1.711 "	508	0.270	326	281
6	3.212 "	508	0.499	322	397
	4.137 "	508	0.635	322	476
	1.854 "	372	0.203	315	298
	3.293 "	385	0.276	322	418
7	3.868 "	393	0.454	323	466
	4.063 "	396	0.481	325	473
	4.410 "	505	0.672	326	534
	3.690 "	507	0.570	323	472
8	3.221 "	515	0.508	323	423
	2.315 "	515	0.366	321	313
	1.743 "	508	0.273	319	291
	7.763 "	416	0.856	334	829
	5.992 "	414	0.705	326	664
9	4.861 "	411	0.575	324	560
	4.328 "	407	0.506	324	519
	3.793 "	403	0.441	323	469
	3.551 "	394	0.399	323	423
	3.284 "	396	0.370	323	408
10	3.033 "	395	0.341	323	402
	2.644 "	392	0.296	325	366
	2.115 "	386	0.233	325	316

TABLE I (cont'd)

Test No.	Reynolds number R_2 based on mass flow, blade dimensions, effective gas temperature	Effective gas temp. T_g °K	Outlet Mach number M_2	Mean blade temperature T_b °K	Nusselt number Nu based on profile + tip + ½ root platform area, blade chord, effective gas temperature
	3.380 × 10^5	512	0.514	325	415
	2.750 "	518	0.430	324	371
11	2.328 "	519	0.359	323	341
	1.956 "	521	0.303	322	306
	1.670 "	523	0.259	322	272
	4.283 "	519	0.661	327	474
	4.255 "	518	0.656	335	483
12	4.291 "	519	0.662	341	485
	4.288 "	519	0.662	312	469
	2.010 "	514	0.312	328	298
	2.078 "	507	0.318	339	310
13	2.090 "	507	0.320	317	310
	2.128 "	503	0.322	324	317
	4.000 "	606	0.714	325	445
	3.222 "	604	0.622	327	418
14	1.879 "	624	0.361	324	279
	2.278 "	624	0.439	327	327
	4.177 "	613	0.775	332	461
	3.881 "	610	0.728	330	438
15	3.396 "	621	0.655	326	409
	3.034 "	620	0.590	329	381
	3.396 "	624	0.650	331	391
	3.132 "	624	0.602	329	383
16	2.616 "	617	0.502	329	347
	2.097 "	628	0.410	328	296
	2.430 "	624	0.471	328	322
	2.096 "	623	0.405	326	298
17	1.635 "	628	0.319	326	255
	1.205 "	630	0.237	326	216
	1.387 "	632	0.272	325	245
18	0.955 "	623	0.184	323	210
	4.523 "	619	0.808	338	671

FIG. 1.

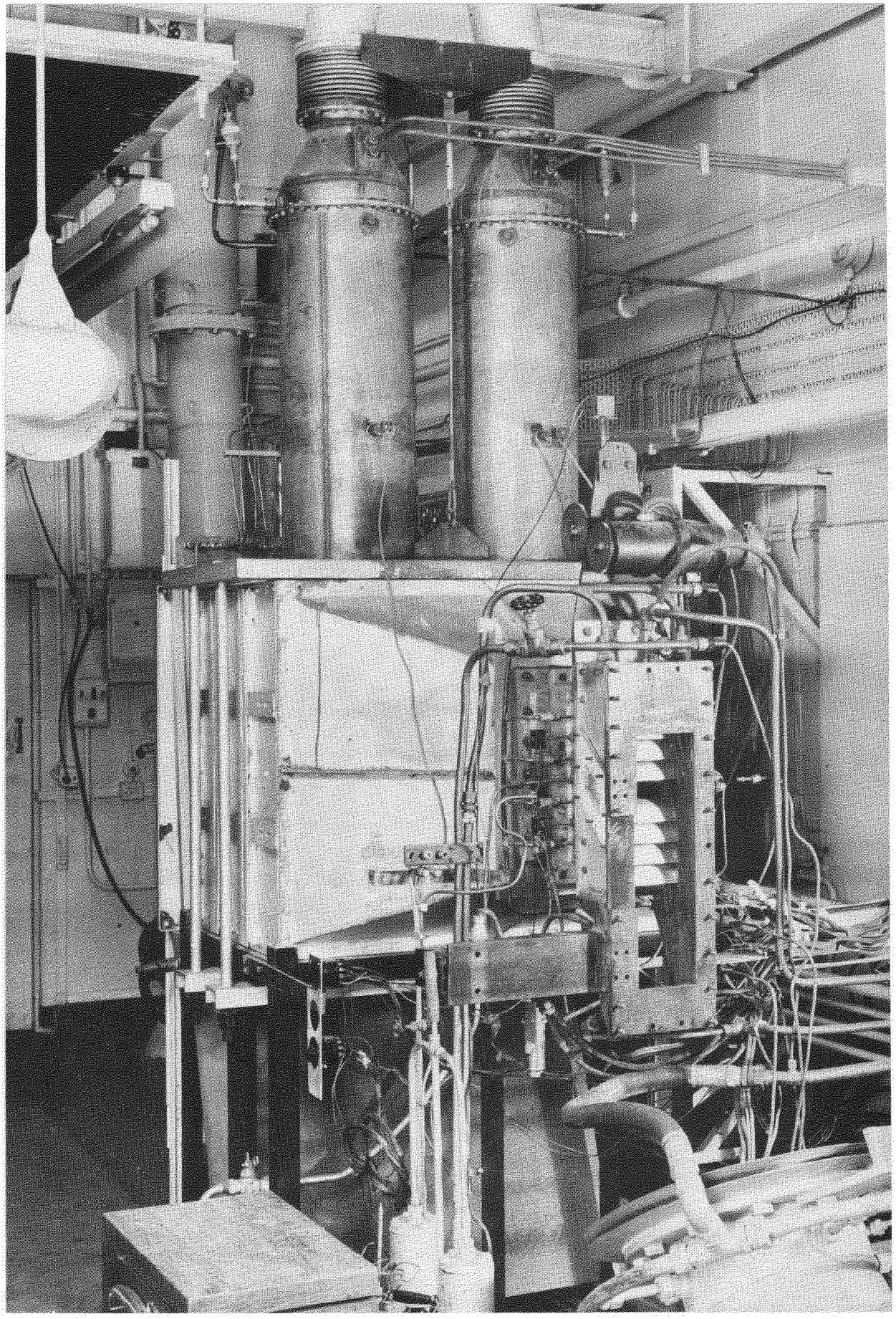

FIG. 2.

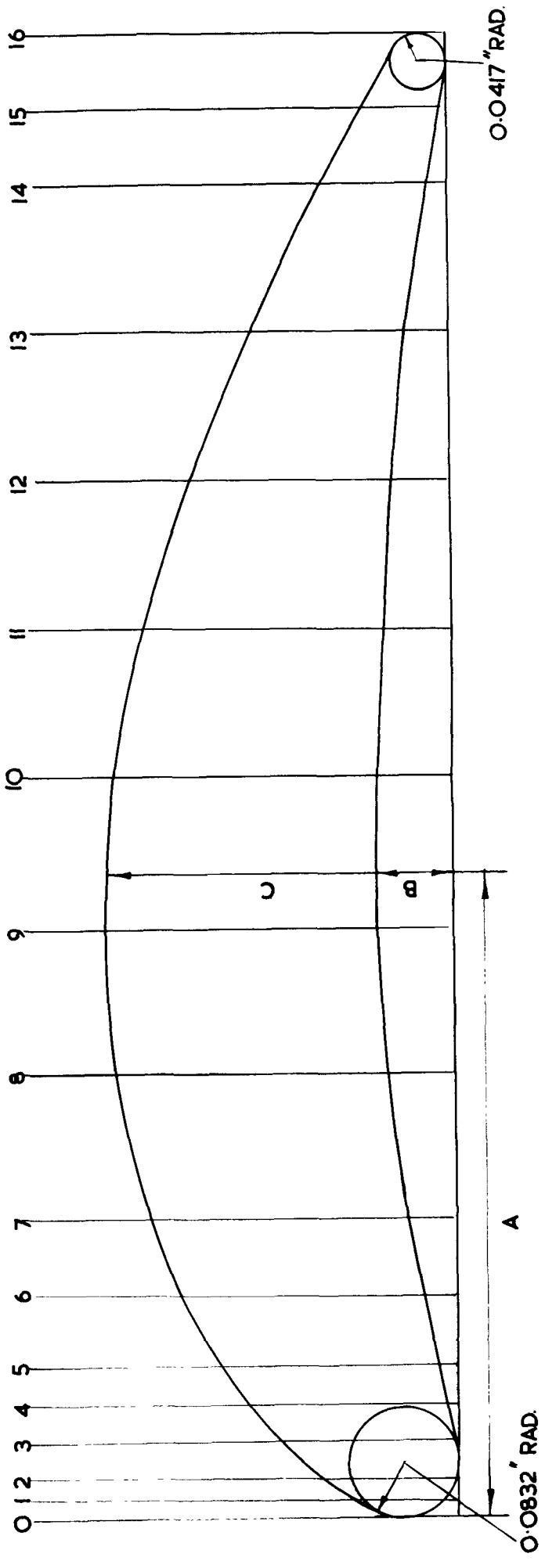

STATION	0	1	2	3	4	5	6	7	8	9	10	11	12	13	14	15	16
A	0	·0283	·0567	·1133	·1700	·2266	·3400	·4533	·6800	·9066	1·1332	1·360	1·5865	1·8132	2·04	2·1532	2·2665
B	·0847	·0210	·0048	·0037	·0127	·0232	·0498	·0727	·1015	·1137	·1102	·1005	·0858	·0618	·0315	·0130	·0435
C	·0847	·1578	·2002	·2670	·3160	·3562	·4180	·4612	·5175	·5295	·5133	·4688	·3960	·3027	·1927	·1305	·0435

BLADE PROFILE

FIG. 3.

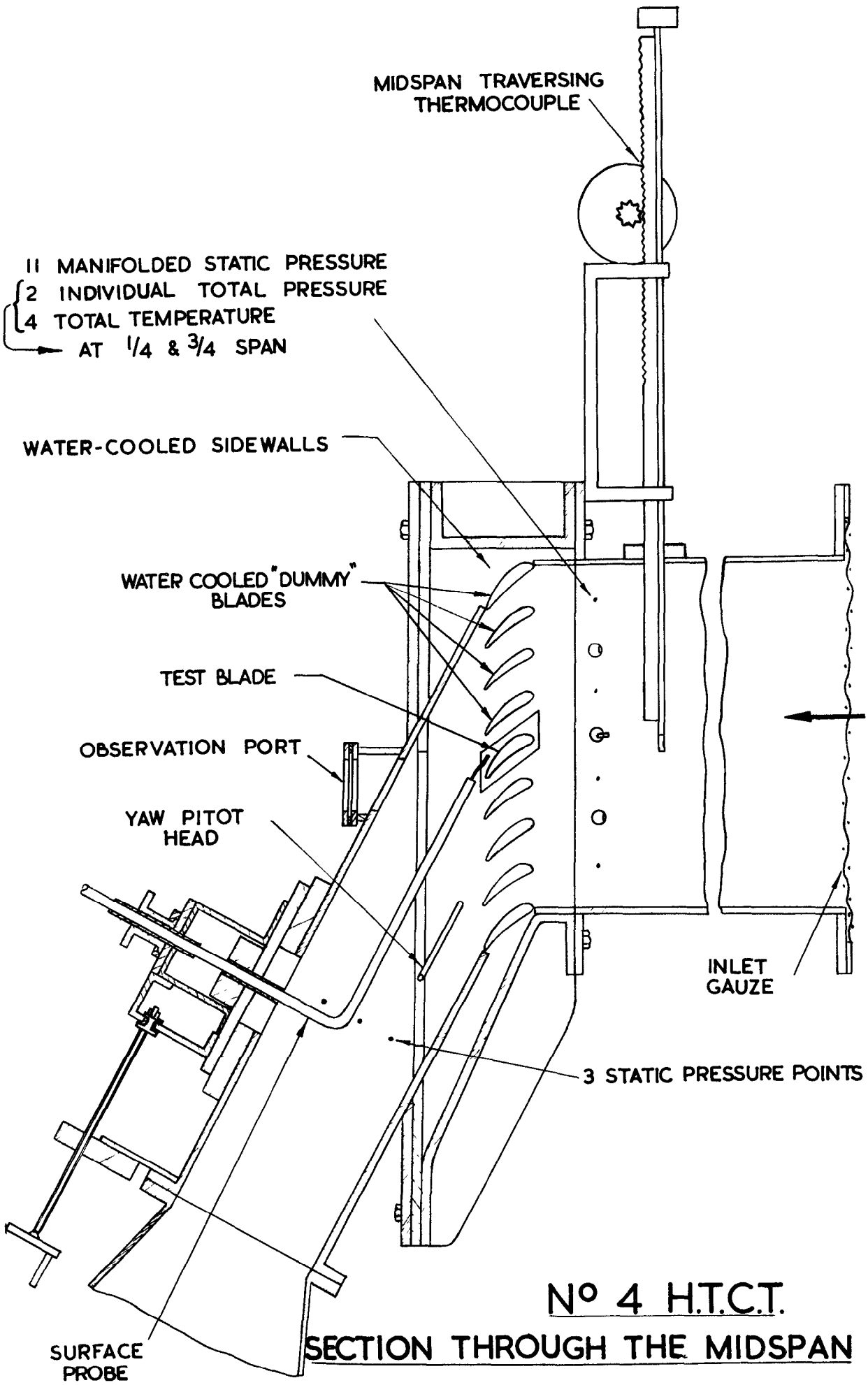

Nº 4 H.T.C.T.

SECTION THROUGH THE MIDSPAN

FIG. 4.

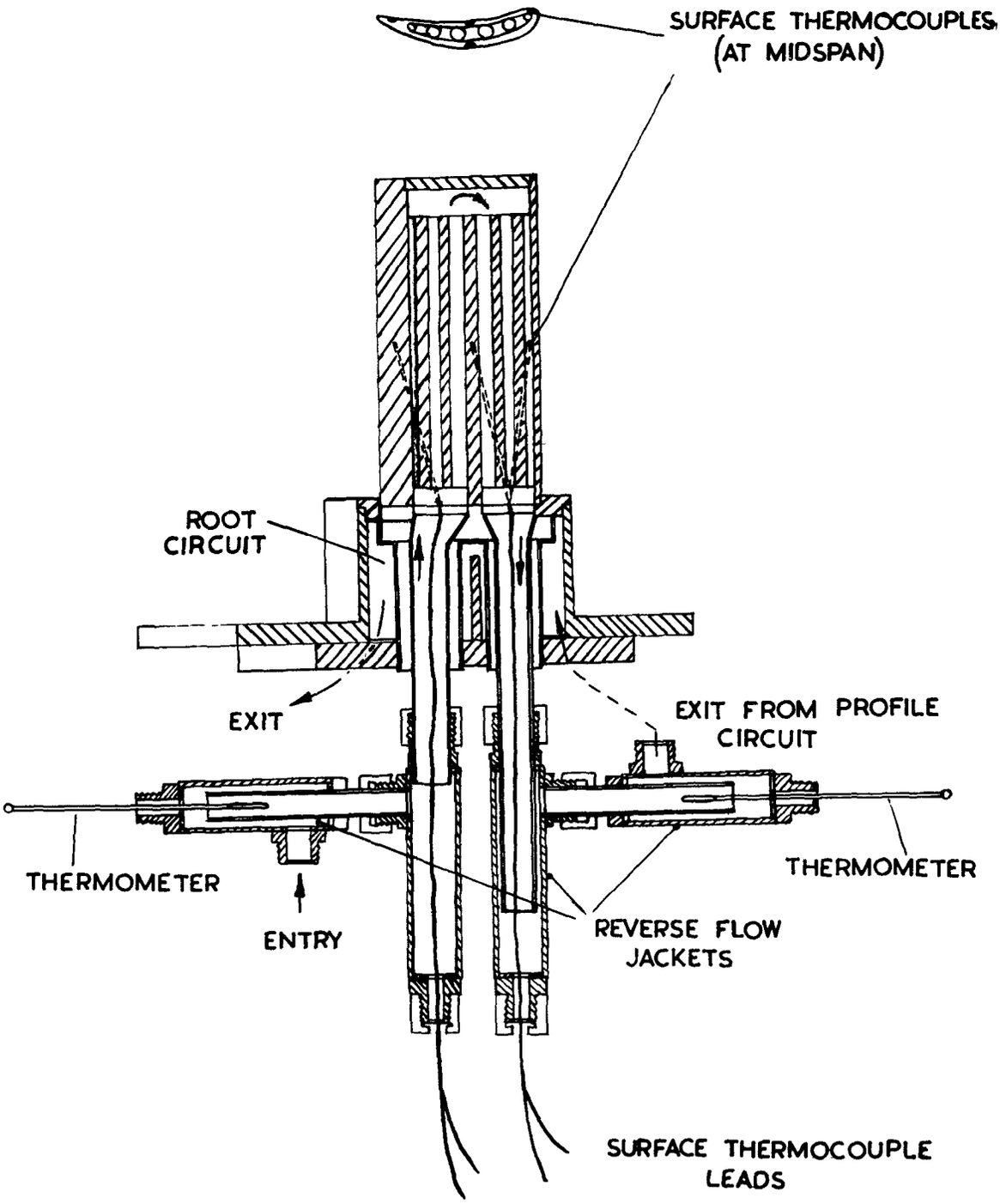

HEAT TRANSFER TEST BLADE

FIG. 5.

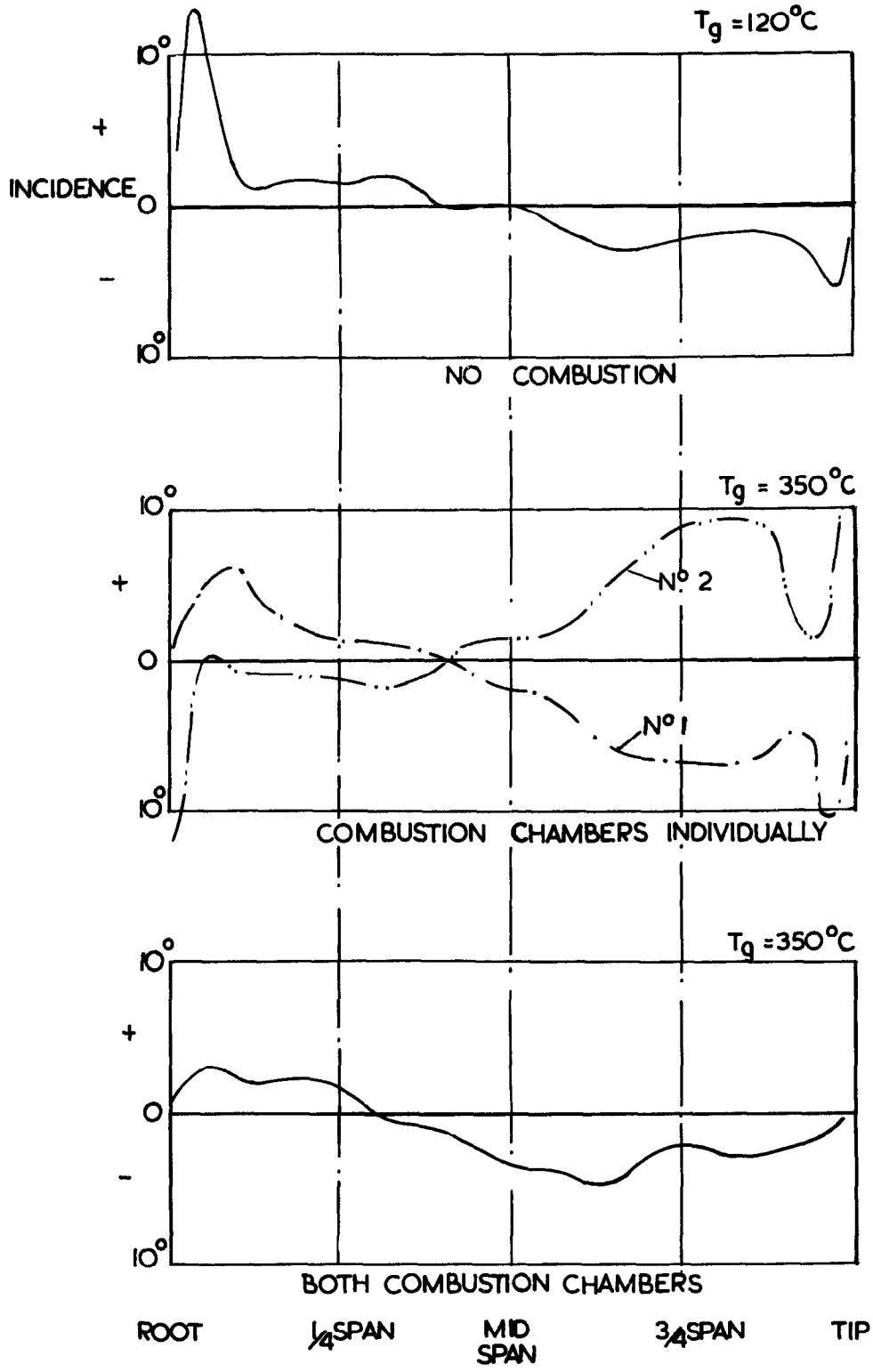

ENTRY GAS INCIDENCE DISTRIBUTION
($M_2 \simeq 0.77$)

FIG. 6.

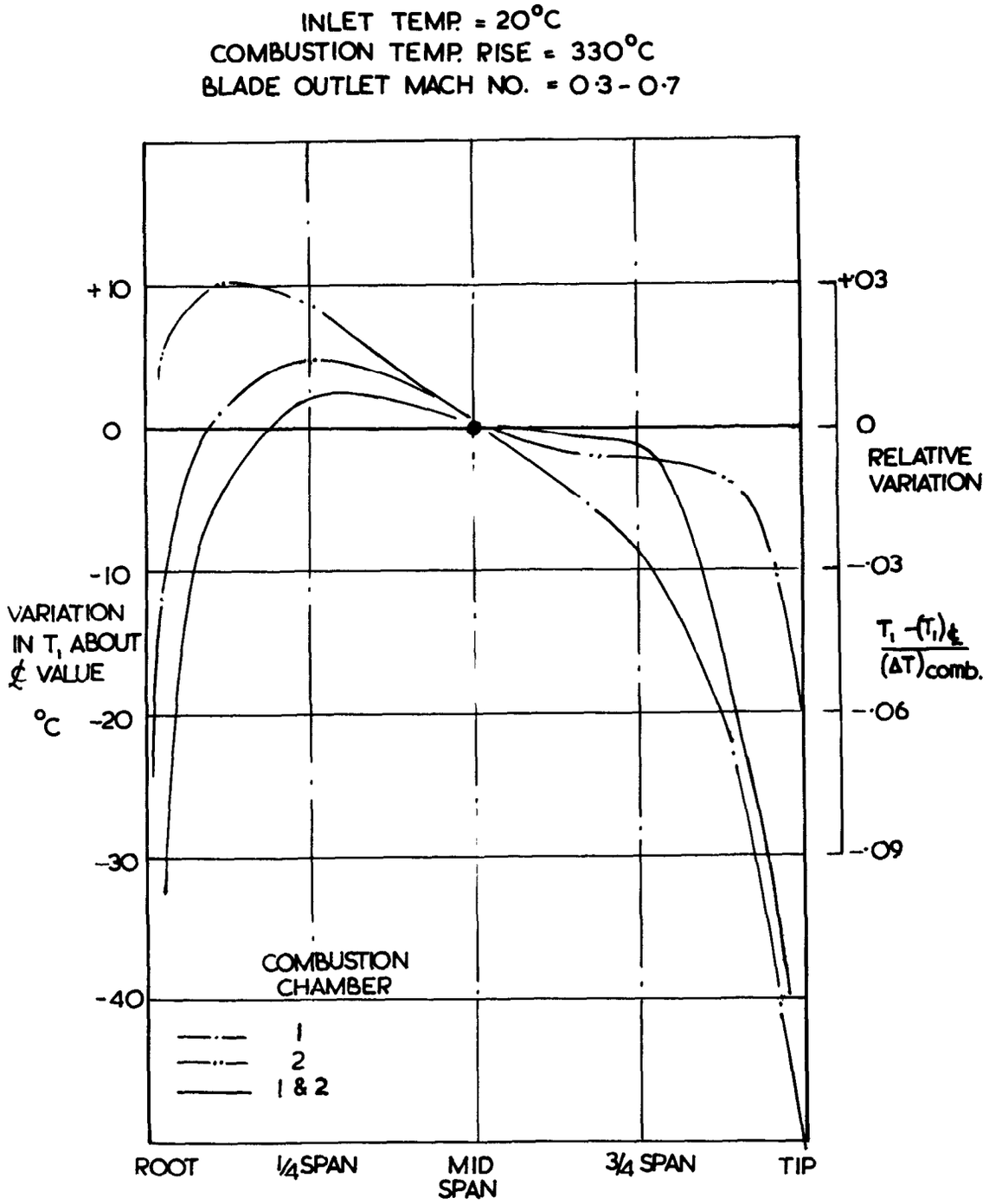

ENTRY GAS TEMPERATURE DISTRIBUTION

FIG. 7.

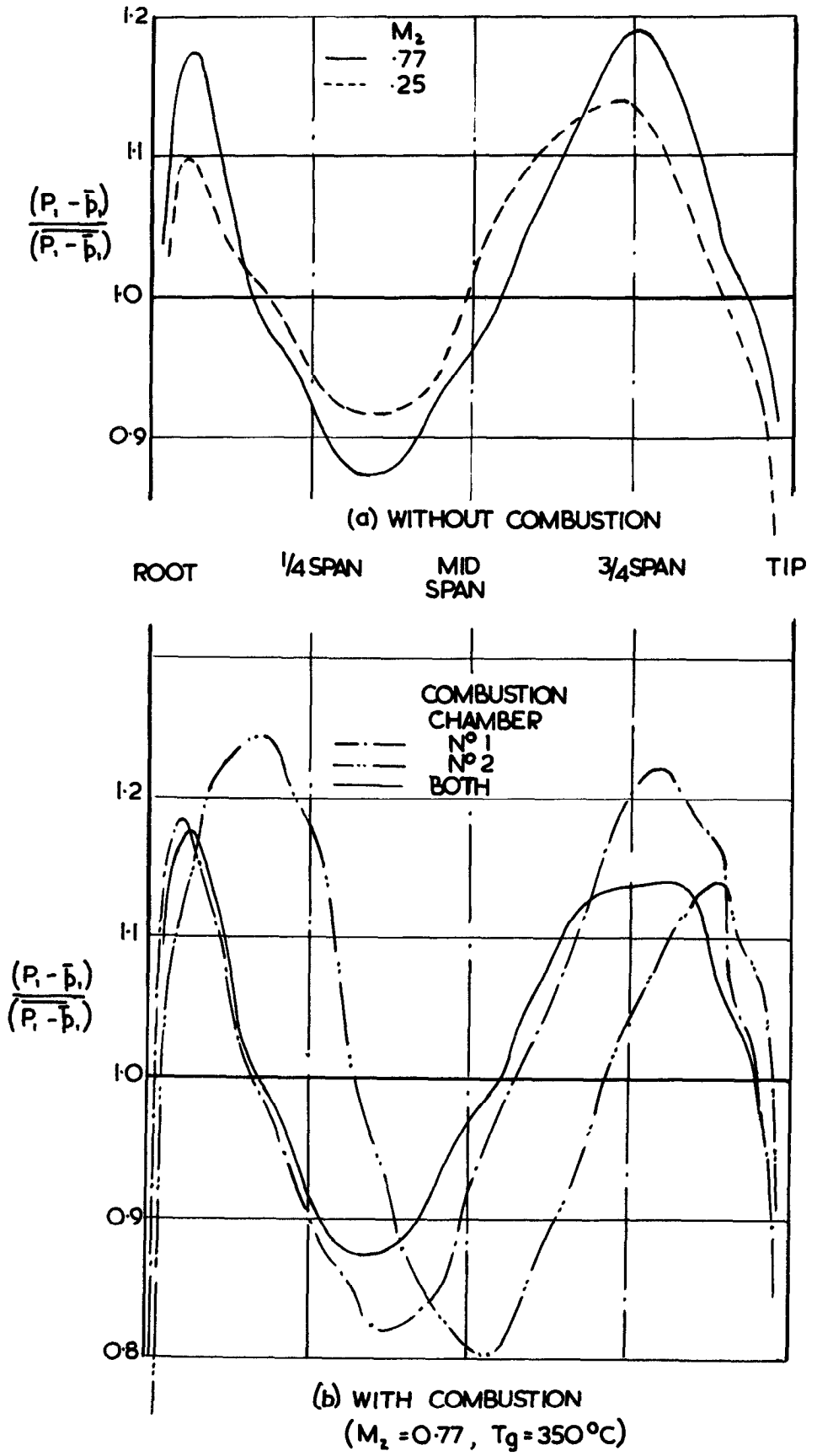

ENTRY TOTAL PRESSURE DISTRIBUTION

FIG. 8.

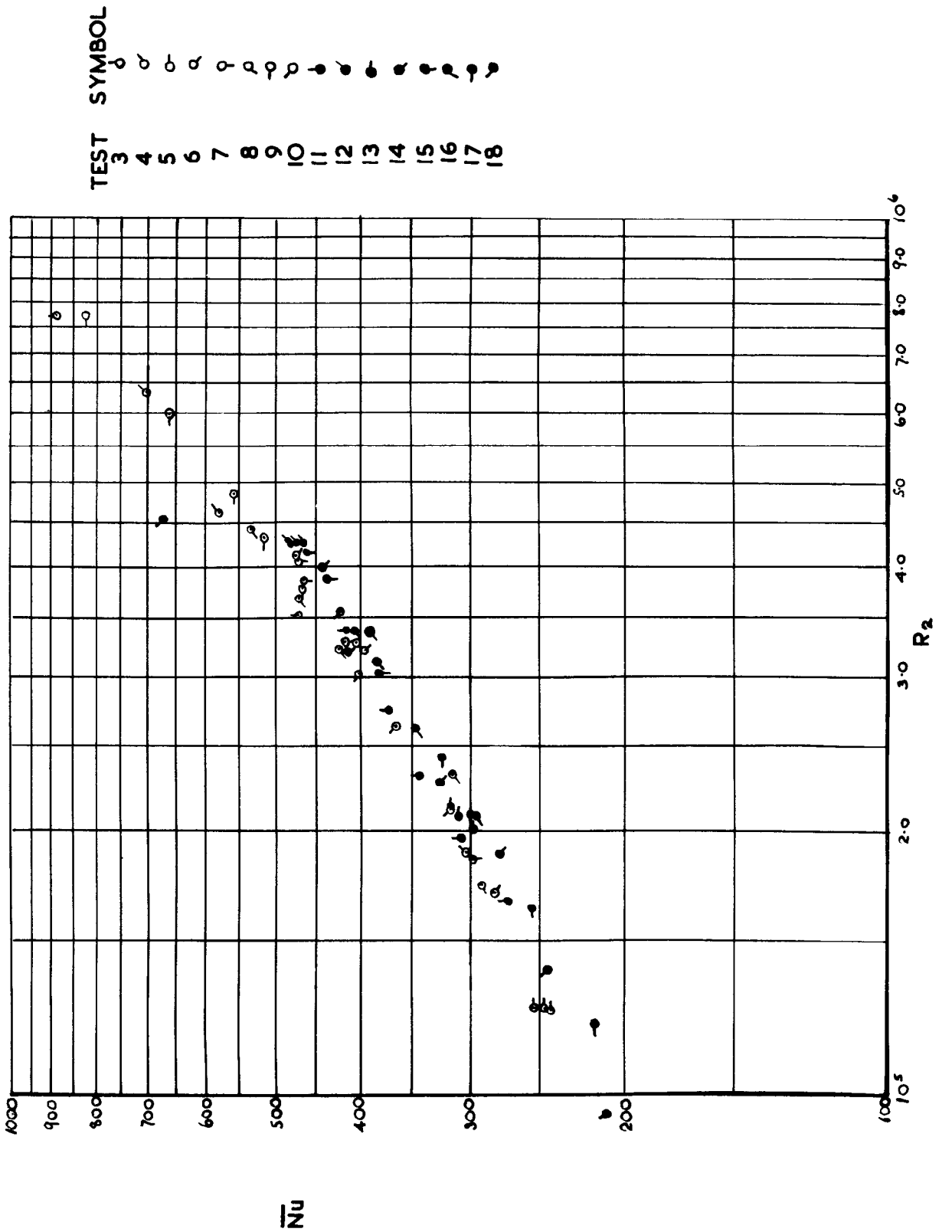

HEAT TRANSFER TEST RESULTS

FIG. 9.

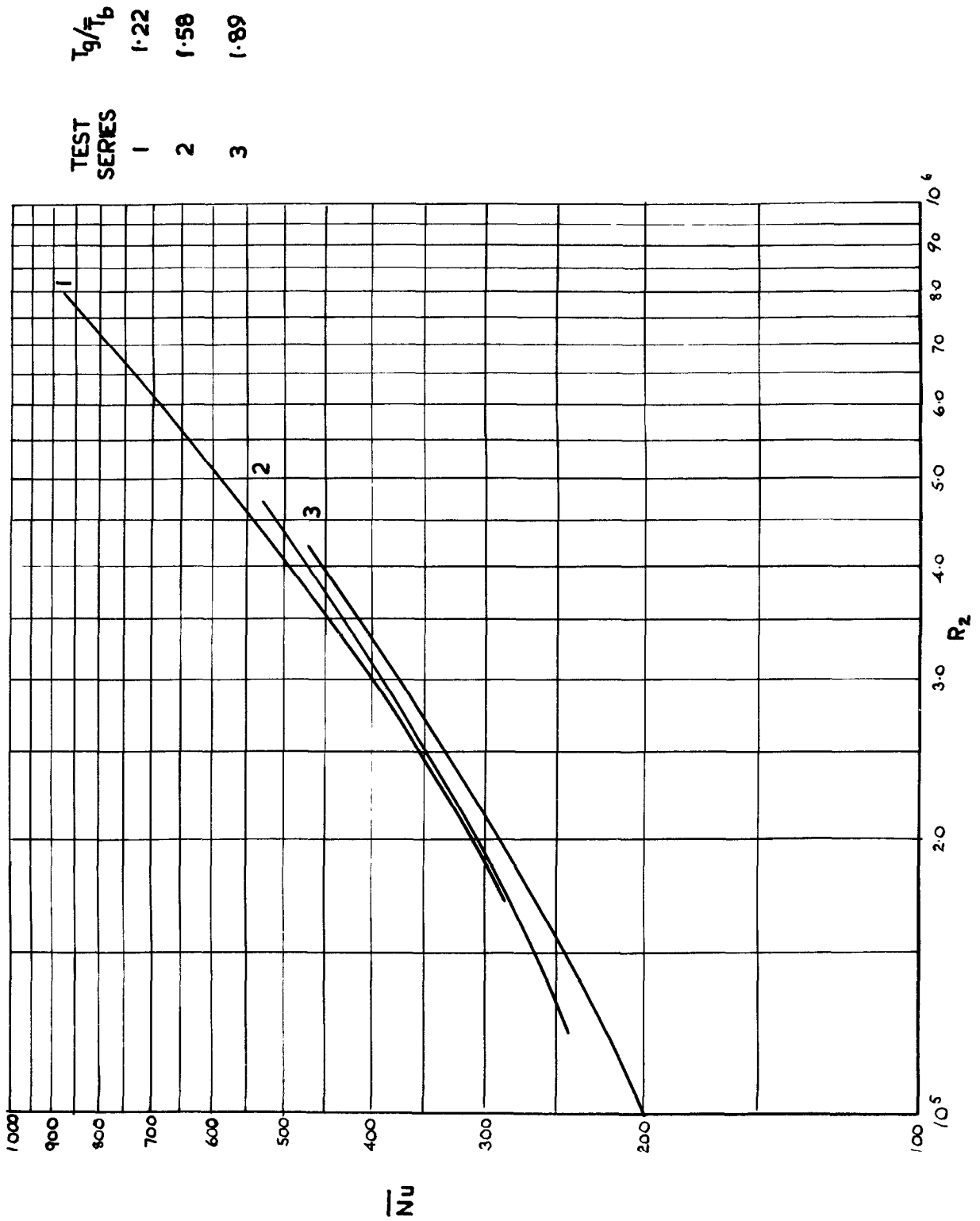

BEST LINES FOR 3 TEMPERATURE RATIOS

FIG. 10.

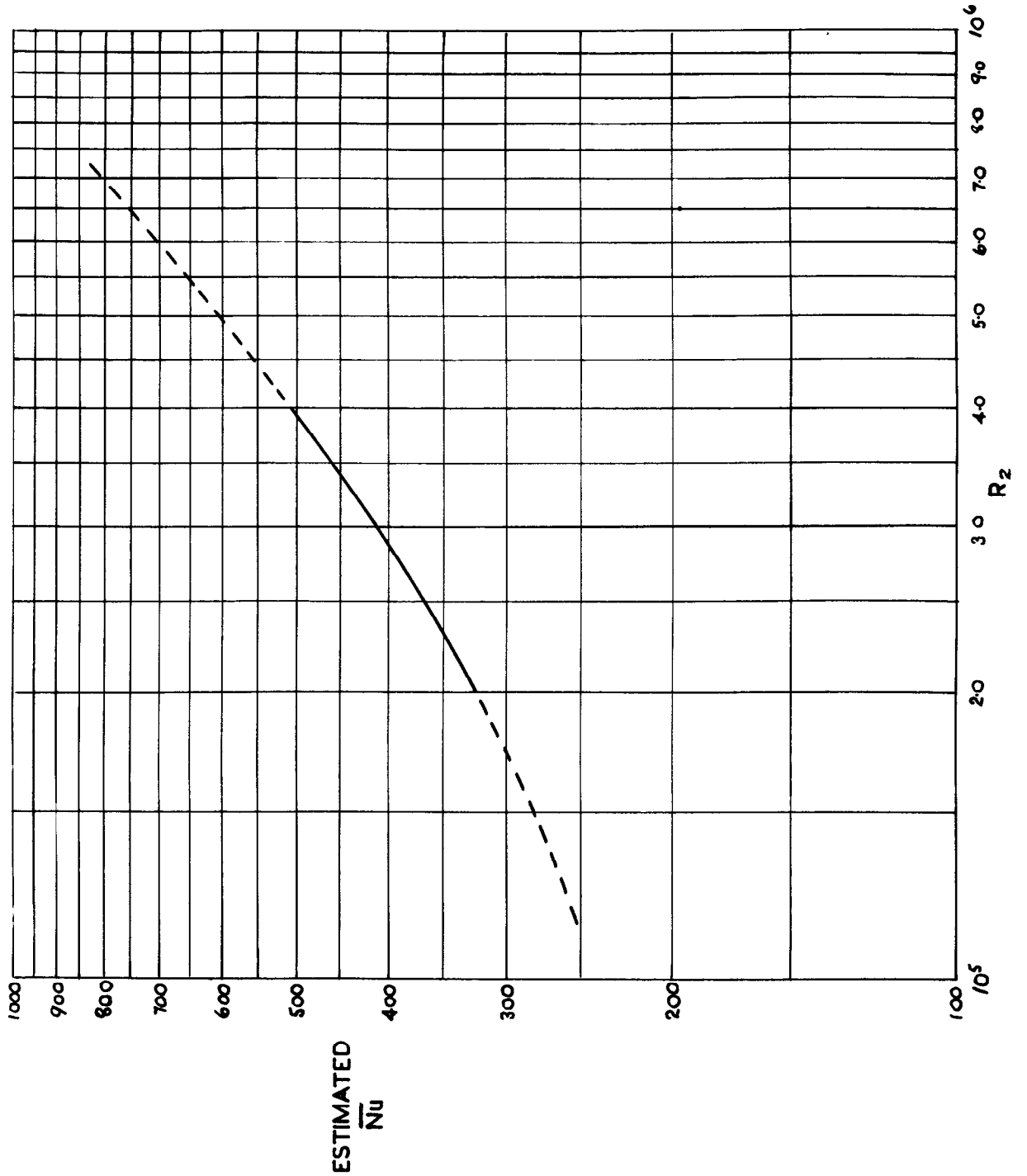

HEAT TRANSFER COEFFICIENT FOR $T_g/T_b = 1$

DS74792/1 Wt60 K4 4/60 CL

C.P. No. 492
(20,361)
A.R.C. Technical Report

Printed and published by
HER MAJESTY'S STATIONERY OFFICE

To be purchased from
York House, Kingsway, London W.C.2
423 Oxford Street, London W.1
13A Castle Street, Edinburgh 2
109 St. Mary Street, Cardiff
39 King Street, Manchester 2
Tower Lane, Bristol 1
2 Edmund Street, Birmingham 3
80 Chichester Street, Belfast 1
or through any bookseller

Printed in England

S.O. Code No. 23-9011-92

C.P. No. 492